*Geophys. J. Int.* (2004) **157,** 1217–1232 doi: 10.1111/j.1365-246X.2004.02247.x

# Analysis of the reliability and resolution of the earthquake source history inferred from waveforms, taking the Chi-Chi earthquake as an example

Shiyong Zhou,[1] Kojiro Irikura[2] and Xiaofei Chen[1]

[1] *Computational Geodynamics Laboratory, Department of Geophysics, Peking University, Beijing* 100871, *China. E-mail: zsy@pku.edu.cn*
[2] *Disaster Prevention Research Institute, Kyoto University, Uji, Kyoto* 611-0011, *Japan. E-mail: irikura@egmdpri01.dpri.kyoto-u.ac.jp*

Accepted 2004 January 25. Received 2003 November 19; in original form 2002 October 18



## SUMMARY

In the inversion of observed waveforms to obtain the earthquake source faulting process some uncertain factors may influence the reliability of the results. Several numerical tests have been analysed in this paper in order to understand the effect of some of these uncertain parameters, such as the number and width of multiple time windows that define the source–time function, the assumed strike and dip of the fault, the velocity structure, and noise. Also, the influence of the sampling rate, the time window of the data and the distribution of observational stations is studied. Our research indicates:

(1) The near-source waveform data can adequately recover the source rupture process of the shallow part of the fault. However, they poorly constrain the slip distribution on the deep part of the fault. Using near-source and teleseismic waveform data jointly can provide a more complete view of the rupture process of the whole fault.

(2) The result using near-fault data is very sensitive to the assumed strike and dip parameters of the fault model. A 2° deviation of the presumed strike and a 5° deviation of the presumed dip from that of the true fault will lead to a distorted inversion result.

(3) The influence of the uncertainty of the seismic velocity structure for the Chi-Chi earthquake might be ignored if we can take the difference between Ma *et al.*'s model and Wu *et al.*'s model as the measure of the media uncertainty.

**Key words:** faulting, numerical techniques, seismic modelling, seismic waves, slip inversion, strong ground motion.

## 1 INTRODUCTION

One of the principal goals in seismology is to infer the nature of the earthquake source from the observed seismograms. Undoubtedly, the seismograms excited by the source contain more information about the source rupture process than any other geophysical data, so matching the observed seismograms is the main way to invert for the source rupture process. Inverting for the earthquake source rupture process by matching waveforms has advanced considerably over the past two decades. Many characteristics of the source rupture, such as nucleation, multiple subfaulting processes, asperities and so on have been revealed via waveform inversions (e.g. Shibazaki *et al.* 2001; Ide 2001; Okada *et al.* 2001; Sekiguchi & Iwata 2002). With the recent improvement of seismic observational techniques and networks, more and more seismologists are focusing their attention on the inversion of the seismic records for the earthquake source rupture processes. The rupture process for almost all of the disastrous earthquakes that have occurred during the past 10 yr, such as the Landers earthquake in 1992, the Loma Prieta earthquake in 1989, the Kobe earthquake in 1995, the Turkey earthquake in 1999, the Chi-Chi earthquake in 1999, and so on, have been studied in this way. Some of these events have been studied several times by different authors with different waveform data or different inversion algorithms. Reading these papers carefully, we find that, even for the same earthquake, the results of inversions by different authors are usually different because of the influence of some uncertain factors. This leads to a question: on what basis can one judge the reliability and precision of the inversion results?

On the other hand, some seismologists who study the earthquake source dynamic evolution problem take the kinematic inversion results inferred from the waveforms as the input data to deduce the dynamic source parameters or dynamic rupture features (e.g. Bouchon 1997; Bouchon & Ihmle 1999; Dalguer *et al.* 2001a,b). So, a reliable and precise kinematic inversion input is very important for such research.

The reliability and precision of waveform inversion for the earthquake source rupture process has been investigated previously. Hartzell (1989) discussed the influence on the inversion results of

the inversion algorithms and the initial models. Beroza & Spudich (1988) discussed the influence of data noise. Sekiguchi *et al.* (2000) analysed the robustness of their inversion results for the 1995 Hyogo-ken Nanbu earthquake and examined the influence of random noise and uncertain velocity structure. Graves & Wald (2001) analysed the resolution of the finite fault source inversion using 1-D and 3-D Green's functions and also discussed the influence of the inexact velocity structure.

The primary goal of this paper is to investigate the influence of some uncertain factors, including the fault model parametrization, the velocity structure and data time windows. We also examine the trade-off between the model parametrization and resolution of the inverted source rupture process. Unfortunately, it has always been difficult to evaluate the resolution and accuracy of the recovered source rupture process in practical cases because we generally do not know the true source history (Wald & Heaton 1994). To avoid this problem, we design a known earthquake faulting model and use a set of synthetic data excited by this 'earthquake' to recover its original faulting process. The consistency between the inversion results and the pre-designed faulting model can indicate the reliability and resolution of the inversion results. The basic procedure we use is: (1) prescribe a source model, observational network and velocity structure; (2) use a forward simulation (Chen 1993, 1999) with the prescribed source model, observational stations and velocity structure to calculate a set of synthetic seismograms as the 'data'; (3) use different data sets and various source parametrizations to invert for the source rupture process and analyse the influence of the uncertain factors by comparing the resulting rupture process with the prescribed source model.

## 2 TEST CASE AND INVERSION METHODOLOGY

### 2.1 Prescribed source model for the test case

In order to place the analysis in a realistic context, we take the 1999 Chi-Chi earthquake as the test case to analyse the reliability and precision of waveform inversion for the earthquake source history. According to the surface breaks along the Chelunpu fault generated by the Chi-Chi earthquake, we simply set the fault plane of the prescribed model as 110 km along strike by 40 km down-dip (from the surface), with a strike of 3°, and a dip of 29° (Lee *et al.* 2000; Ma *et al.* 2001). The hypocentre of the Chi-Chi earthquake is located 30 km along strike and 16.5 km down-dip from the southern top corner of the rectangular fault. Similar to the test case of Graves & Wald (2001), we design the slip distribution of the prescribed model by two simple rectangular slip patches (asperities). The slip on the northern asperity is a constant 5 m and the slip on the southern asperity is a constant 2 m, which approximates the slip distribution recovered for the Chi-Chi earthquake by some authors (Yagi & Kikuchi 2000; Ma *et al.* 2001; Zeng & Chen 2001). The rupture time distribution of the prescribed model is taken as a uniform propagation with a constant rupture velocity of 2.5 km $s^{-1}$. For simplicity, we set a constant rake of 85° and a cosine slip velocity source–time function with 3.0 s duration as expressed by:

$$\dot{s}(t) = \begin{cases} \dfrac{1-\cos(2\pi t/R)}{R} & \text{for} \quad 0 \le t \le R \\ 0 & \text{for} \quad t = \text{others} \end{cases} \tag{1}$$

where $\dot{s}(t)$ is the slip velocity source–time function and $R$ is the source rupture duration which is prescribed as 3.0 s in our test case. Fig. 1 illustrates our prescribed source model for the tests.

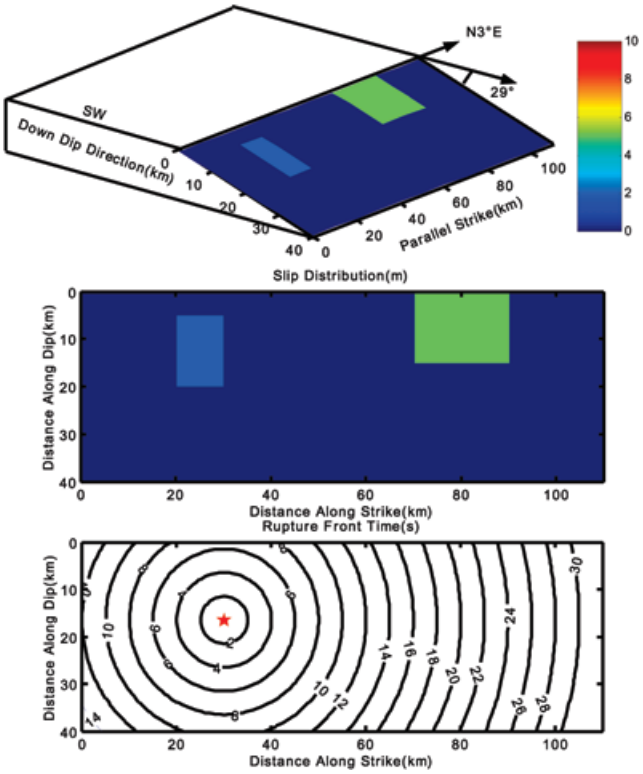


**Figure 1.** Prescribed source model. The hypocentre is marked by ⋆.

According to the site investigation by the Taiwan Central Geological Survey (Chen *et al.* 2001), the seismogenic fault of the Chi-Chi earthquake is much more complex than our prescribed fault model and may consist of several segments with different strike and dip angles. The slip distribution, rupture propagation and source–time function are also more complex than the prescribed source model. However, since our primary goal in this paper is to examine the possibility of inverting for a reliable and precise earthquake source rupturing process using traditional methods, taking a simple prescribed source model as the test case is the clearest way to study the robustness of the inversion results. We will use a more complex fault model when we use our newly developed inversion method (Zhou & Chen 2003) to invert for the rupture process of the Chi-Chi earthquake in a future study.

Fig. 2 shows the 21 near-source stations and the velocity structure used to generate the 'observational data' in our test case. The locations of the stations are listed in Table 1. The velocity model is the average velocity structure of western Taiwan as inferred from the work of Change *et al.* (2000) and Chen *et al.* (1998). The 21 stations are the stations which best recorded the Chi-Chi earthquake, among about 600 local digital accelerometers (Lee *et al.* 2001), and are widely used in inversion studies of the Chi-Chi earthquake (Ma *et al.* 2001; Wu *et al.* 2001; Zeng & Chen 2001). We will use the generalized reflection/transmission method developed by Chen (1993, 1999) to calculate the 'data' in our numerical tests. The sampling and the length of each data record will be described in detail in the following section.

### 2.2 Inversion methodology

During the past two decades, many methods have been developed to invert for the earthquake rupture process from seismic

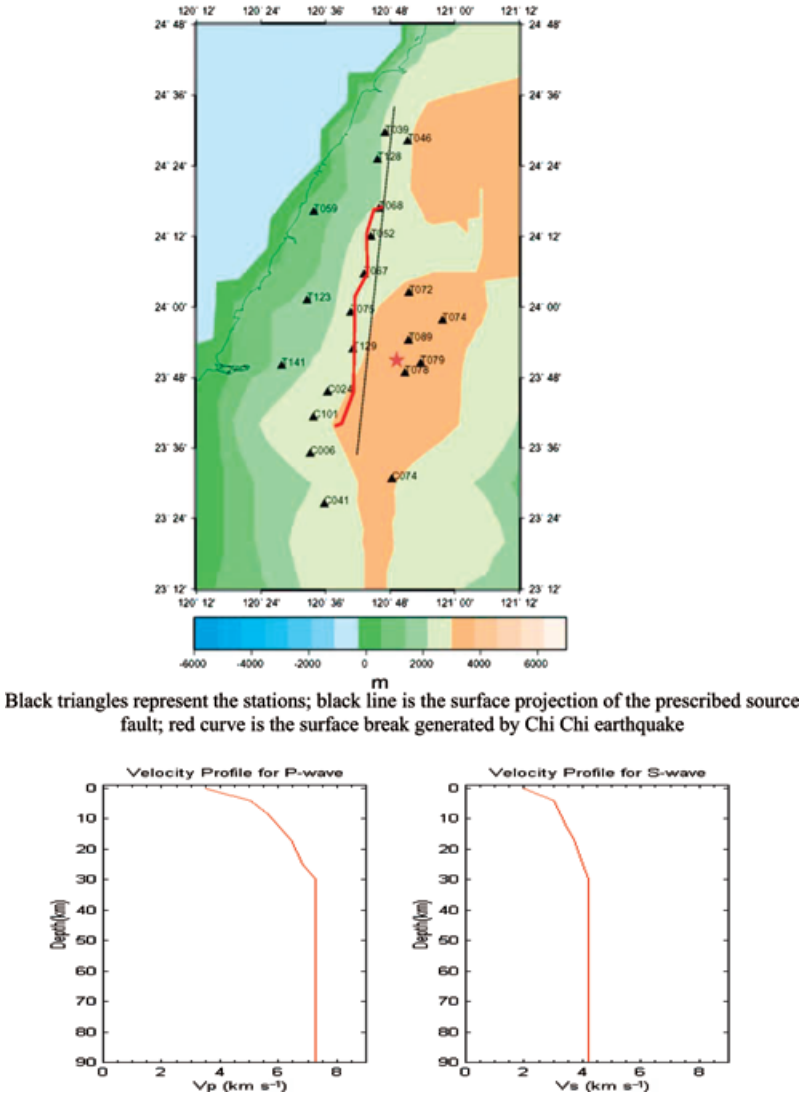


Black triangles represent the stations; black line is the surface projection of the prescribed source fault; red curve is the surface break generated by Chi Chi earthquake

**Figure 2.** Distribution of the strong motion stations and the regional media structure.

waveform data. These methods can be divided into two approaches. In one, the slip and rupture time are recovered simultaneously, such as in the linearized method (e.g. Beroza & Spudich 1988; Zhou & Chen 2003), in the frequency-domain inversion method (e.g. Olson & Anderson 1988), or in the global statistical search optimization method (e.g. Fukuyama & Irikura 1986; Zeng & Anderson 1996; Hartzell & Liu 1996; Ji *et al.* 2001). The main advantage of this approach is that both the slip and rupture front time distribution on the fault can be determined simultaneously. The main disadvantage is that the mathematical expression of the source–time function is usually assumed. Dynamic faulting research based on both seismic observations and rock rupturing experiments (Ohnaka & Yamashita 1989; Miyatake & Yamashita 1995; Nakumura & Miyatake 2000) and numerical simulations (Day 1982; Dalguer *et al.* 2001b) show that the earthquake source–time function is very complex. It may vary at different points on the fault, and cannot be described with a simple functional form. The other main approach is the multiple time-window inversion, which was presented initially by Olson & Apsel (1982). After their pioneering work, much progress has made this inversion method more sophisticated (Hartzell & Heaton 1983; Hartzell 1989; Nakayama & Takeo 1997; Sekiguchi *et al.* 2000). Both methods discretize the fault surface into a set of cells (or subfaults). The second requires the pre-setting of several temporal segments (multitime windows) for each cell. This is done so that each cell on the fault may slip within any of these time windows in order to accommodate the complexity of the slip functions and model variations in rupturing front times (effectively allowing the rise time and rupture velocity to vary spatially). The basic inversion equation of this method (Hartzell 1989) can be expressed as a simple linear optimization problem:

$$\begin{pmatrix} wG \\ \lambda S \end{pmatrix} X \cong \begin{pmatrix} wd \\ 0 \end{pmatrix} \text{ s.t. } X >= 0.0 \tag{2}$$

where $G$ is the matrix of Green's functions and $d$ is the data vector of observed seismic waveforms. $S$ is a matrix of smoothing constraints, where the difference between the slip on adjacent subfaults is set to zero. $\lambda$ is a linear weight, whose magnitude controls the trade-off between satisfying the constraints and fitting the data. $w$ is the inverse value of the corresponding observational data point, thus normalizing the data and letting all the recordings with different values have the same weight when fitting the waveforms. Sekiguchi *et al.* (2000) introduced Akaike's Bayesian information

**Table 1.** Location of the stations.

| Name of station | Code | Latitude (°) | Longitude (°) |
|---|---|---|---|
| T039 | Sta1 | 24.4922 | 120.7838 |
| T046 | Sta2 | 24.4687 | 120.8540 |
| T052 | Sta3 | 24.198 | 120.740 |
| T059 | Sta4 | 24.2688 | 120.5637 |
| T067 | Sta5 | 24.0917 | 120.7197 |
| T068 | Sta6 | 24.278 | 120.7657 |
| T072 | Sta7 | 24.0392 | 120.8577 |
| T074 | Sta8 | 23.9607 | 120.9617 |
| T075 | Sta9 | 23.9835 | 120.6778 |
| T078 | Sta10 | 23.8123 | 120.8455 |
| T079 | Sta11 | 23.8397 | 120.8942 |
| T089 | Sta12 | 23.9037 | 120.8565 |
| T123 | Sta13 | 24.0177 | 120.5427 |
| T128 | Sta14 | 24.4162 | 120.7607 |
| T129 | Sta15 | 23.8783 | 120.6843 |
| T141 | Sta16 | 23.8335 | 120.4640 |
| C006 | Sta17 | 23.5822 | 120.5522 |
| C024 | Sta18 | 23.7577 | 120.6065 |
| C041 | Sta19 | 23.4393 | 120.5957 |
| C074 | Sta20 | 23.5103 | 120.8052 |
| C101 | Sta21 | 23.6862 | 120.5622 |
| RAYN | Sta22 | 23.52 | 45.5 |
| CTAO | Sta23 | 20.09 | 146.26 |
| KBS | Sta24 | 78.93 | 11.94 |

criterion (ABIC) (Akaike 1980) to select the appropriate smoothing weight λ.

The main advantage of this method is that the form of the source–time function need not be presumed but is instead described by the combination of a series of temporal basis functions (such as a triangle function) with different weights. Each of these basis functions is localized within one of the pre-set multiple time windows, which can overlap each other. So, the source–time function is nearly an arbitrary function. If we have inverted for the slip weight for a particular subfault within its own time window in eq. (2), we can easily recreate the source–time function of the subfault. Fig. 3 illustrates the way to obtain the source–time function. Theoretically, if we pre-set the number of the multitime windows for each subfault large enough (i.e. the interval between the neighbouring time windows is small enough), it is possible to invert for a complex faulting process with variable rupture propagation and arbitrary source–time function. However, a large number of multitime windows means that more unknown parameters are contained in the inversion eq. (2), which requires more data. Because we have abundant seismograms for the Chi-Chi earthquake, it is possible to use the multiple time-window method to invert for the faulting process without constraining the form of the source–time functions. The following analysis in this paper will mainly use the multiple time-window method.

The NNLS (non-negative least square) algorithm was recommended by Hartzell (1989) to solve the multitime window inversion problem described by eq. (2). Householder transformations are applied in this algorithm to avoid taking the product $G^{\mathrm{T}}G$, which would lead to a squaring of the singular values of the matrix and a loss of accuracy. However, we prefer to choose the Gauss iteration algorithm with non-negative constraint for several reasons:

(1) The Gauss algorithm needs less memory than NNLS. This is because NLLS needs to use a sequence of Householder transformations to convert an asymmetrical matrix to a upper triangularized Heisenberg matrix and needs to use QR (singular value decomposition) to get eigenvalues and eigenvectors. So there are dual iteration processes in NNLS. In the Gauss algorithm only a mono-iteration process is required.

(2) It is true that Householder transformations avoid taking the product $G^{\mathrm{T}}G$ in NNLS. However, for an ill-conditioned matrix inversion problem the solution might be unstable. This originates from the problem itself instead of the algorithm because the solution is unique for a linear matrix inversion problem. For a deterministic problem, the unstable solution originates from the rounding errors of the digital operations. Such an unstable phenomenon should be more serious in NNLS since there are many more operations needed for calculating the matrix inversions.

### 2.3 Source parametrization

The parametrization of the source is a key step in the waveform inversions. It is one of the main tasks in our paper to examine how the parametrization influences the inversion results. The parametrization in the multitime window method mainly includes: (1) the discretization of the fault surface; (2) discretization of the source–time function (the number of multitime windows, and the basis function of the source–time function); and (3) an assumed rupture propagation velocity. The discretization of the fault surface generally depends on how much detail we want to know about the source process and on how good/numerous the waveform data are. Sekiguchi *et al.* (2000) discussed the problem of discretization of the fault surface. They pointed out that the spatial periodicity arising from discretization of the fault was likely to generate spurious synthetic waves of the corresponding frequency. They suggested that the subfault size should be carefully chosen to make the dominant frequency caused by the spatial periodicity lie outside the frequency range of the used waveform data. We discretize the fault into 704 (44 × 16) identical subfaults, each with a dimension of 2.5 km by 2.5 km. The spatial periodicity arising from our discretization is more than 1.5 Hz,

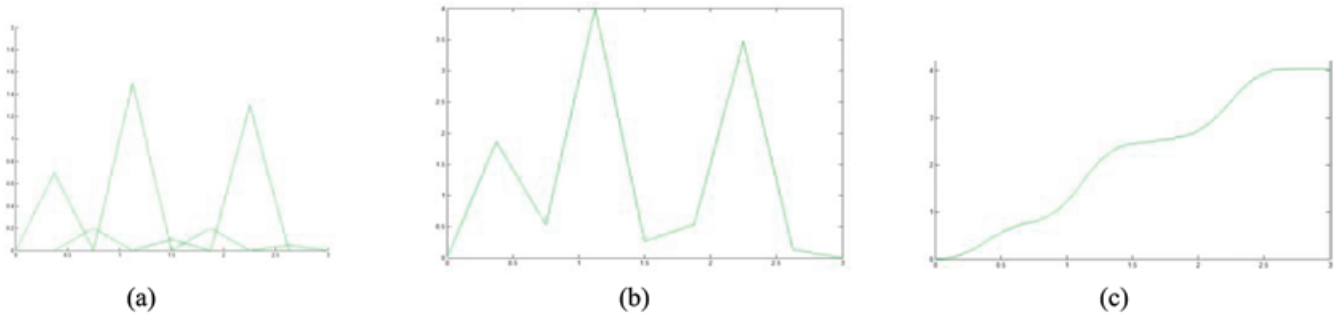


**Figure 3.** Schematic illustration of combining the multi-overlapped triangle functions with different weights into a source–time function.

**Table 2.** Parameters of the finite fault source inversion.

| | |
|---|---|
| Discretization of the fault | 2.5km × 2.5 km for each subfault<br>The fault plane is discretized into 704 subfaults totally |
| Basic function for the source–time function discretization | $\frac{1-\cos(2\pi t/w)}{w}\frac{4}{w^2}\begin{cases} t & 0 \le t < 0.5w \\ w-t & 0.5w \le t < w \\ 0 & \text{other} \end{cases}$ |
| The number of multitime windows | 1–12 |
| Possible rupture time range of the incorporated source–time function | −2.0–3.3 |

$w$ is the width of the time window

**Table 3.** Inversion data.

| Data type | Sampling rate (Hz) | Nyquist frequency (Hz) | Hamming filter parameters (Hz) | Length for each record (s) |
|---|---|---|---|---|
| Near-source | 2.5 | 1.25 | For near-source data: | 45.0 |
| | 3.333 | 1.66 | lower freq. 0.1, 0.2; | 70.0 |
| | 2.5 | 1.25 | higher freq. 0.9, 1.0 | 95.0 |
| Teleseismic | 1.0 | 0.5 | For teleseismic data: lower freq. 0.05, 0.1; higher freq. 0.35, 0.4 | 500.0 |

which is outside frequency range (0.1 to 1.0 Hz) of the waveform data used in our research.

In order to compare the inversion results using different discretizations of the source–time function, we consider triangle functions with 0.3 to 1.0 s rise and 0.3 to 1.0 s fall. We also consider a cosine function of 3 s duration. The number of multitime windows is also taken from 1 to 12 for different tests in our study. The neighbouring time windows on each subfault half overlap each other. Table 2 summarizes the various parametrizations of the source we will test in this analysis.

### 2.4 Data

The data used in our test inversions are generated by the generalized reflection/transmission method (Chen 1993, 1999) and have been filtered with a Hamming filter. The parameters of the filter are listed in Table 3. Because the seismogram length of the record and the sampling rate may both affect the resolution of the inversion results, we will use different record lengths and different sampling rates to test their influence. Table 3 lists the data sets we will use in different tests.

## 3 ANALYSIS OF THE RESULTS

### 3.1 Influence from the number of the multitime windows and the length of the data

The number of multitime windows is a parameter that must be assumed when the multitime window algorithm is used to invert for the earthquake faulting process. Another parameter to be considered is the length of the waveform data used in the inversion. In the following inversion tests, the same source–time function, the same fault parameters (the strike, dip and the size of the fault) and the same velocity model as those of the prescribed source are used so as to remove any other uncertain factors from our discussion on the effects of the number of the multitime windows and the length of the data.

Fig. 4 shows the inversion results with different lengths of near-source waveform data and different numbers of multitime windows. Because the source–time function and velocity structure used in the calculation of the Green's function matrix $G$ in these inversion tests are the same as those used in the calculation of the 'data' ($d$ vector), and there is no noise, we expected that we could completely recover the slip distribution pattern of the prescribed source model. But instead we find that we cannot completely recover the source if we only use the near-source ground motion data in the inversion.

From Fig. 4, we can see that:

(1) The full waveforms should be used in the inversion for a more reliable recovery of the source rupture process. If shorter waveform record segments are used, the data will contain less information on the more remote and deeper subfaults of the source fault and the slips on those subfaults are poorly constrained. Fig. 5 indicates that the longest duration of ground motion among the 21 stations in our test case was about 80 s.

(2) Although the time-window parametrization can certainly provide the possibility of inverting for a complex source rupture process with variable rupture velocity (an arbitrary source–time function as we mentioned in the introduction), it may also produce some false patterns in the recovered source rupture process because of the trade-off among the slip distribution, rupture front time distribution and source–time functions (Hartzell & Heaton 1983; Hartzell 1989; Wald & Heaton 1994). A larger number of time windows may require more data to constrain the source and reduce such trade-offs.

(3) The slip distribution on the shallow part of the fault can be recovered quite well using the near-source waveforms. However, even when a single time window is used to remove the trade-off between the slip distribution and rupture delay time distribution, there is still a small false slip area on the deeper part of the fault in the inversion result.

To investigate the possible factors which lead to this false slip area, we select some subfaults from three down-dip profiles of the fault and compare the elements of the synthetic Green's function matrix $G$ excited by these subfaults. The synthetics excited by shallow and deep subfaults with the same unit slip are shown in Fig. 6. We can see from the synthetics in Fig. 6 that there is obvious variation in the amplitude of the waveform according to the depth of the subfault. The synthetics from the deep subfaults are much weaker than those from the shallow subfaults, which may be the main reason that the slip distribution on the deep part of the fault is more difficult to recover with the near-source waveforms. We also find that the synthetics from the more remote deep subfaults are the weakest (subfaults 12, 14, 16 in the right column of Fig. 6). Compared with other synthetics, they are so weak that their contribution to the observed ground motions can almost be ignored, which is a plausible reason why a false slip pattern can easily occur on these subfaults.

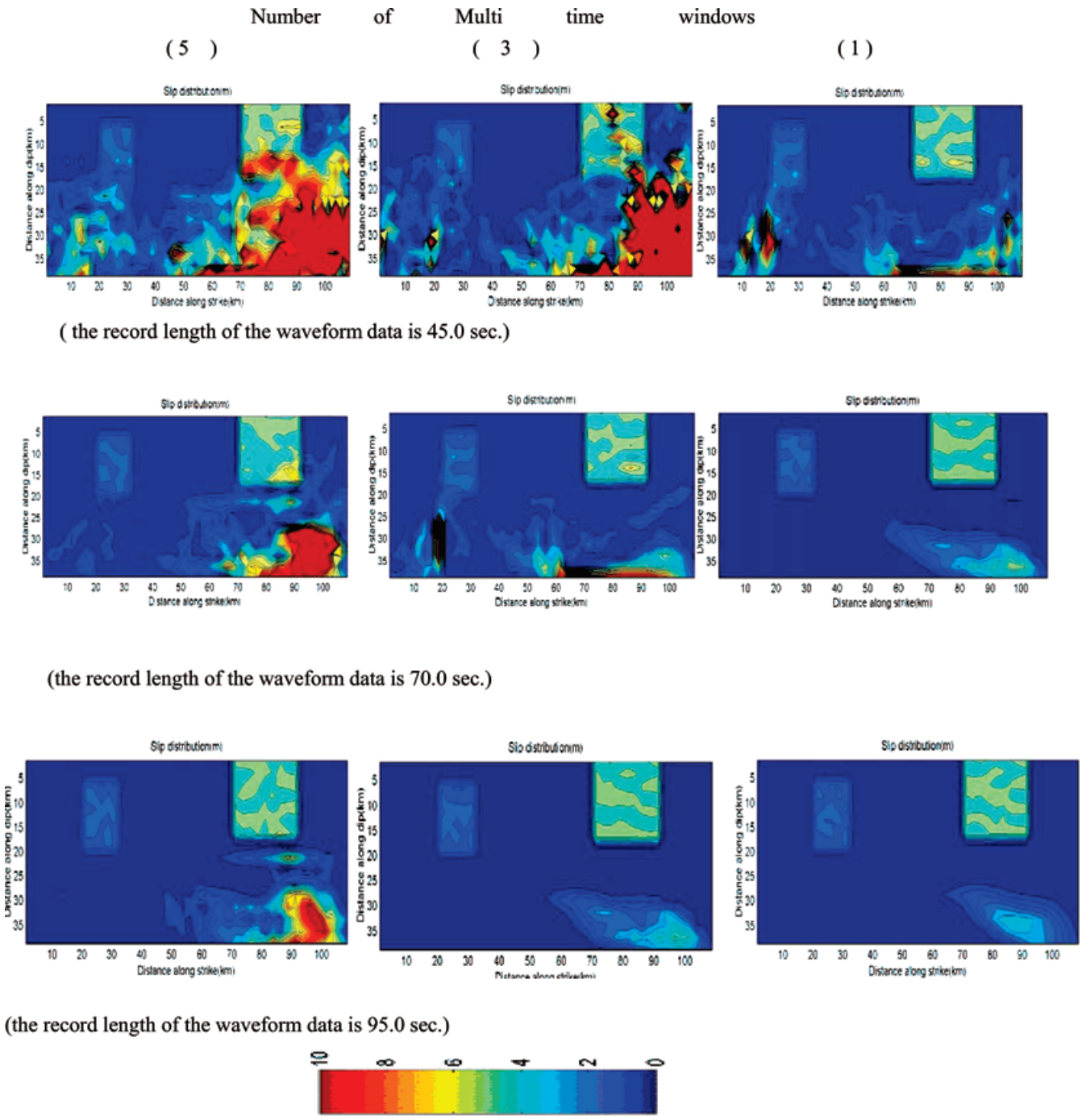


**Figure 4.** Rupture processes inverted with near-source waveform data.

To improve the inversion resolution on the deep part of the source, we add data from one to three GDSN stations (see Table 1) to our tests. Fig. 7 shows the synthetics of the stations excited by some subfaults with different depths. We can see that there is no significant variation in synthetic waveforms with depth, or along strike, which means that the synthetics from all subfaults on the fault have nearly the same contribution to the teleseismic ground motion. So, using the near-source and teleseismic waveform records jointly may improve the inversion resolution on the whole fault. Fig. 8 shows the inversion results using the full waveforms of the 21 near-field stations and the *P* waveform of one teleseismic station. We can see that the source has been perfectly recovered.

### 3.2 Influence of the width of the basis function

The source–time function plays a very important role in the calculation of the synthetic seismograms. In research on source history, we should also invert for the source–time function as we do for the slip and rupture front distribution on the fault. In the multitime window inversion method, the source–time function is temporally discretized and expressed as the linear sum of a series of basis functions with weights (see Fig. 3). Because the iso-triangle function is usually chosen from among all the possible basis functions, such as triangle, ramp, sine or cosine functions (Olson & Apsel 1982; Hartzell & Heaton 1983; Wald & Heaton 1994; Nakayama & Takeo

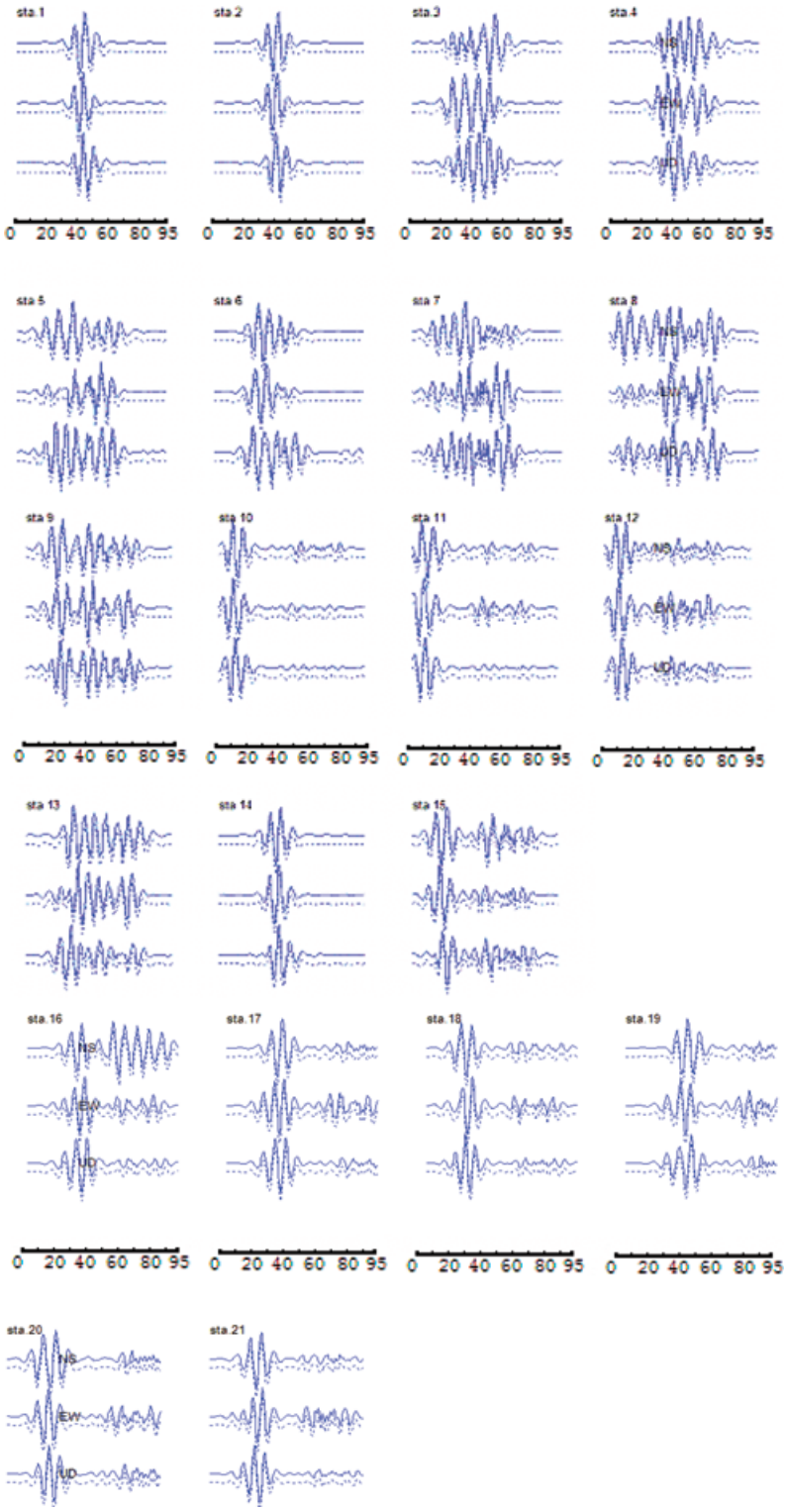


**Figure 5.** Comparison of observation (dashed lines) and synthetics(solid lines) in the inversion with the record length of the waveform data 95.0 s and three time windows.

1997; Sekiguchi *et al.* 2000), we take the iso-triangle function as the basis function in our discussion of the influence of the width of the time window. We take the total time range of the overlapped multitime windows to cover the rise-time duration of the real source to ensure that it is possible to find a perfect source–time function with such a set of basis functions.

To remove the influence of other uncertain factors, the fault parameters (strike, dip and the size of the fault) and the velocity model are taken as those of the prescribed source in the inversion calculations and we use waveforms from both the 21 near-source stations and three teleseismic stations to ensure we have enough data to recover the source history.

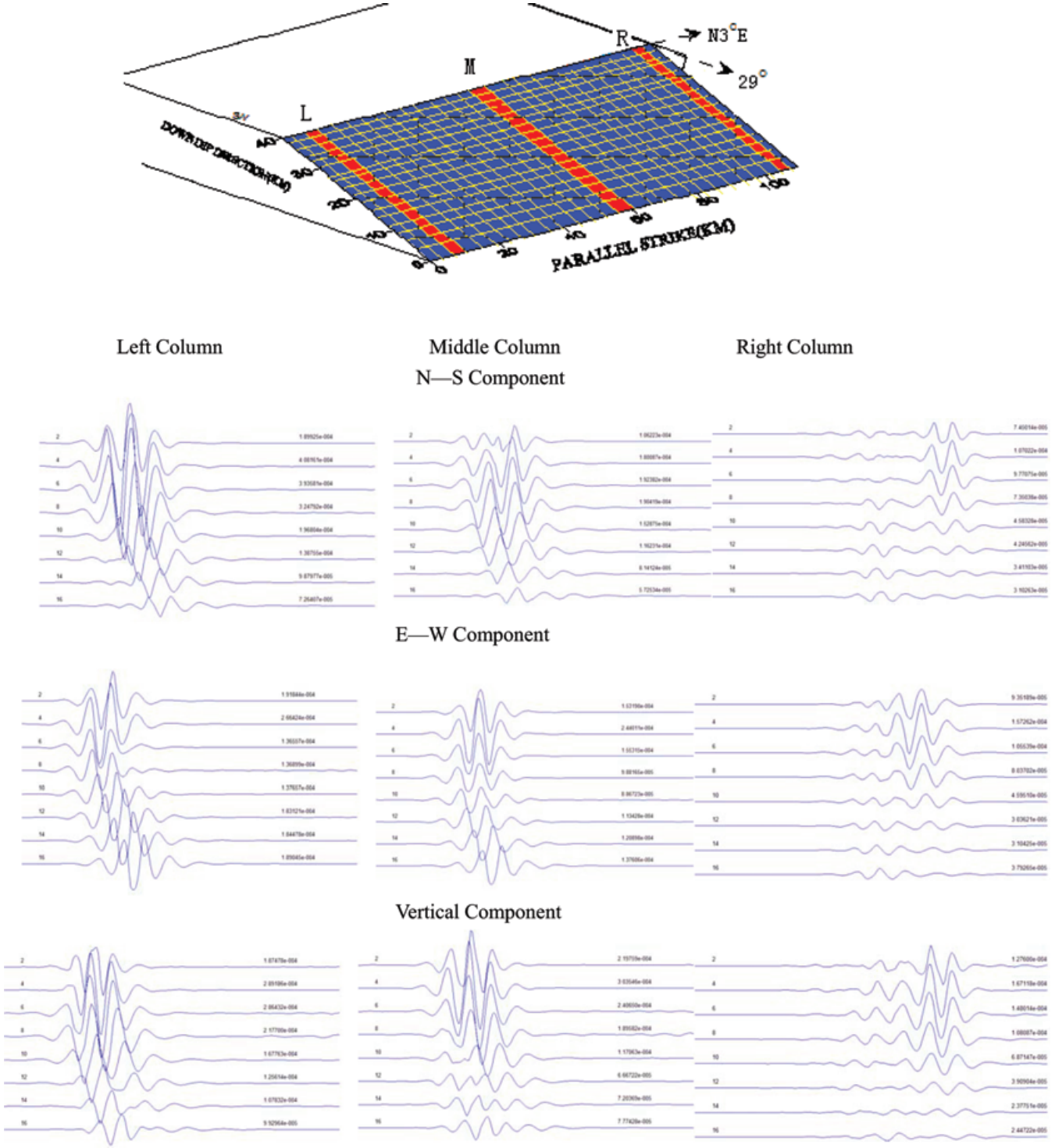


**Figure 6.** Synthetics of the station 10 (T078) for the subfaults with different depths on the three selected dip-ward columns.

Fig. 9 shows the results inverted by four different time window combinations(see Table 4). We can see that: (1) the smaller the width of the time window, the finer the source–time function that could be obtained, and the more accurate inversion result could be achieved; and (2) the spare time windows have little influence on the inversion result when the data used in the inversion are sufficient.

We should point out:

(1) The total time range of the overlapping multitime windows should not be less than the possible maximum rise-time duration of the real source–time function.

(2) A smaller width of the time window is helpful for inverting a finer source history. However, more time windows should be used to ensure that the total time range of the overlapping multitime windows is long enough. Also, higher-frequency data and more

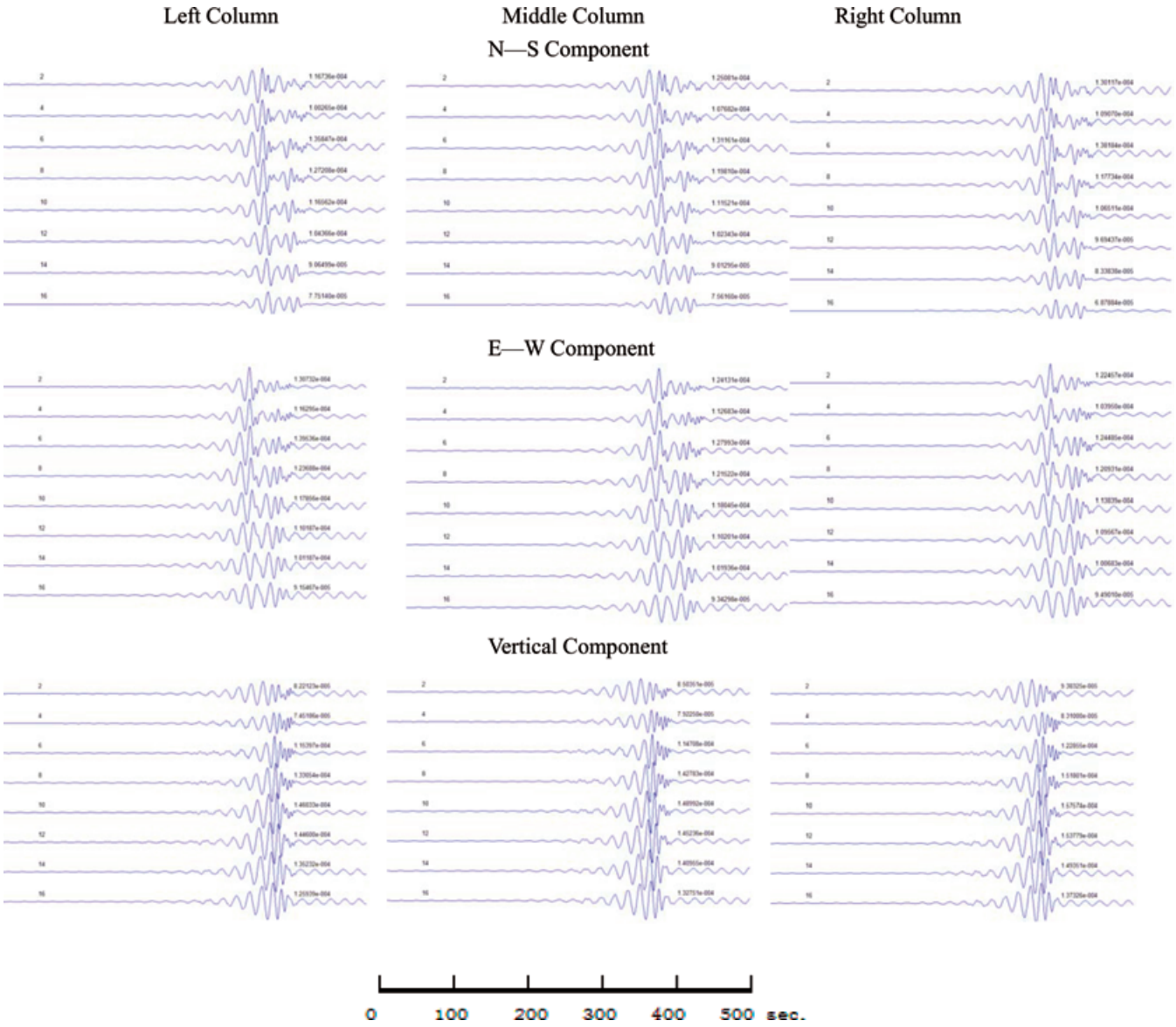


**Figure 7.** Synthetics of the station 24 (KBS) for the subfaults with different depths on the three selected dip-ward columns.

data will be required to ensure there is enough information to obtain a fine inversion of the source history.

(3) A large number of multitime windows will require more expensive computation.

### 3.3 Influence of the uncertain strike or dip of the fault

A very important step in setting up the inversion model is to determine the strike and dip of the rupture plane. At present, a widely accepted method for determining the source mechanism parameters such as strike, dip and slip angle is to invert for them using both teleseismic waveform records and the polarities of *P*-wave initial motions. However, the strike and dip based on moment tensor inversion using teleseismic waveform fitting have errors. Xu (1995) discussed the influence of the uncertainty of the focal depth to the inversion of the earthquake source mechanism parameters, and pointed out that the uncertainty of the strike is about 15° while the uncertainty of dip is smaller, say from 5° to 10°. The parameters inferred from *P* initial motions usually have larger uncertainty. So the strike and dip based on the source mechanism have some uncertainties, which will influence the inversion results.

In order to discuss the effects of the strike or dip discrepancy, we pre-set the departure of the strike and dip of the inversion rupture plane from that of the prescribed model as 15°, 10°, 5°, 2°, or 1°. The inversion results indicate that the strike and dip departure could seriously influence the results and the fittings can be very poor (see Fig. 10). But with the strike and dip getting closer to the true values, the waveform fitting becomes much better, the shape of the area with no rupture becomes clearer and the slip distribution is closer to the prescribed model. This means that it is possible for us to find a best-fitting result by changing the strike and dip. In fact, this idea to how to reduce the influence of uncertainty of the strike and dip on the inversion results has been adopted in inverting the seismic source rupture process using teleseismic records (Ma *et al.* 2001). From Fig. 11, we can see that although the strike and dip of the model only deviates by 1° from the real model, the misfit is

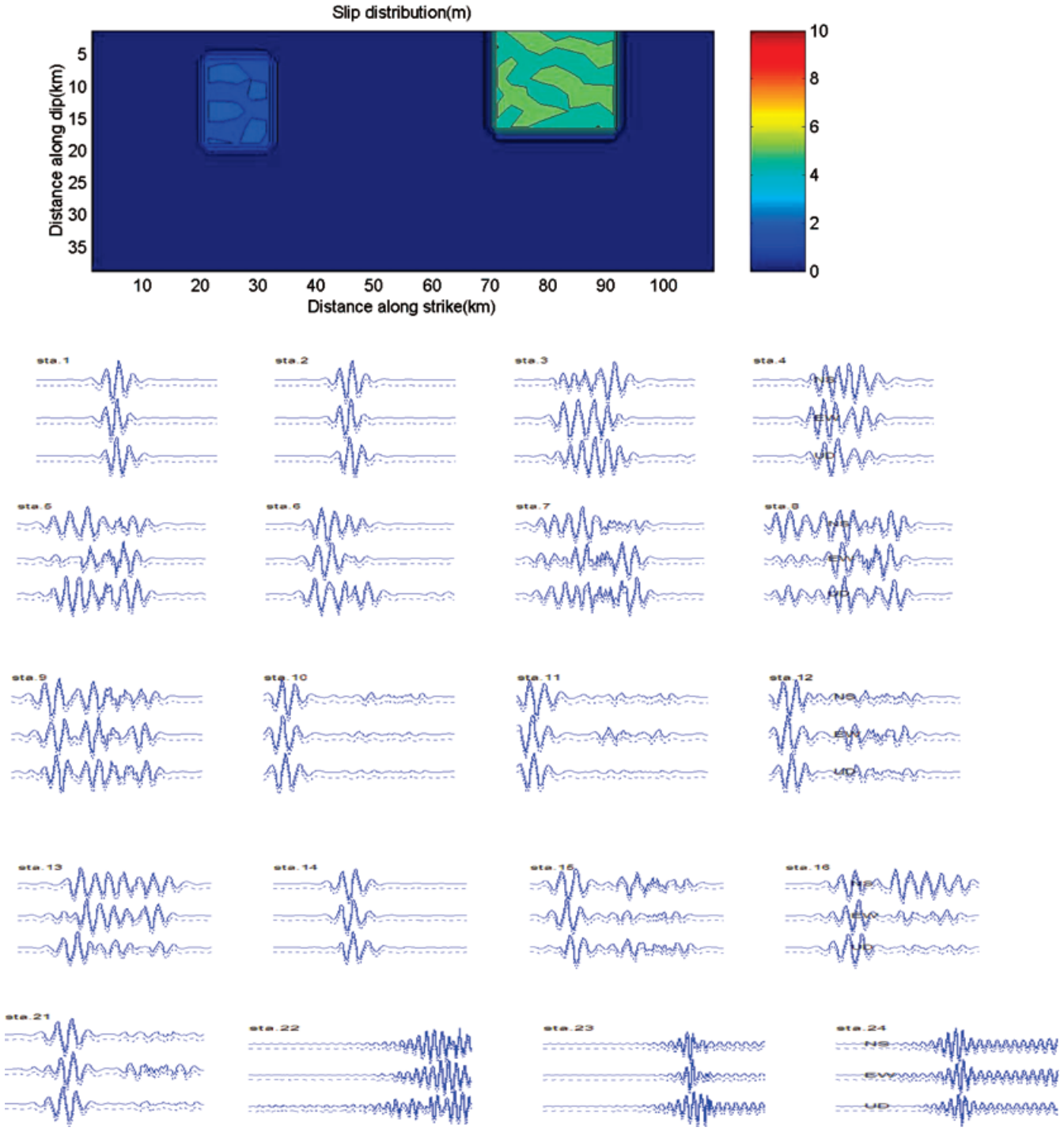


**Figure 8.** Rupture processes inverted both with near-source waveform data and teleseismic data.

still large. So when inverting by use of the near-source waveform records, we can theoretically determine the strike and slip within 1°. However, we must note that in a practical inversion process the noise in the data and the possibly complex shape of the rupture may influence the precision of the strike and dip determinations. Furthermore, we must pay special attention to inversion results using only near-source seismic records when we cannot ensure that the parameters of the pre-set fault are close to those of the real fault of the earthquake.

### 3.4 Influence of an uncertain velocity structure and data noise

There are two kinds of noise. The first kind of noise originates from the data (matrix $d$ in eq. 2) which are often contaminated by white noise. The second originates from the uncertainties of the velocity structure, which may lead to some errors in the calculation of the Green's functions (matrix $G$ in eq. 2). To remove all uncertainties other than the influence of noise, we will make the parameters of

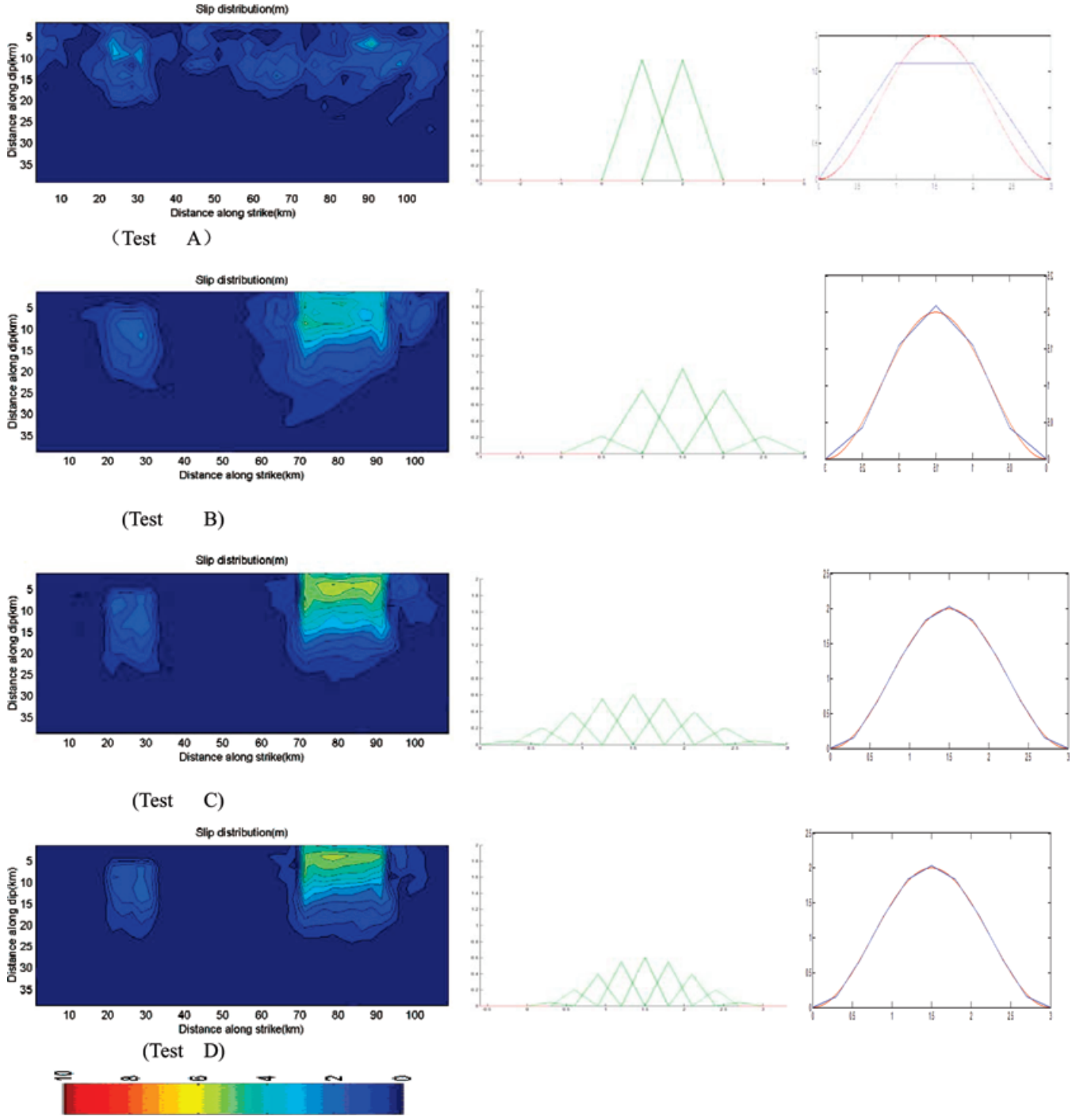


**Figure 9.** Inversion results with different sets of time windows and the perfectly incorporated source–time function by the basic functions.

**Table 4.** The parameters of the time windows we used in our tests.

| Test code | Width of time window (s) | Overlap length of neighbouring windows (s) | Number of time windows | Possible rupture time range of the incorporated source–time function (s) |
|---|---|---|---|---|
| A | 2.0 | 1.0 | 7 | −3.0–5.0 |
| B | 1.0 | 0.5 | 7 | −1.0–3.0 |
| C | 0.6 | 0.3 | 9 | 0.0–3.0 |
| D | 0.6 | 0.3 | 12 | −0.6–3.3 |

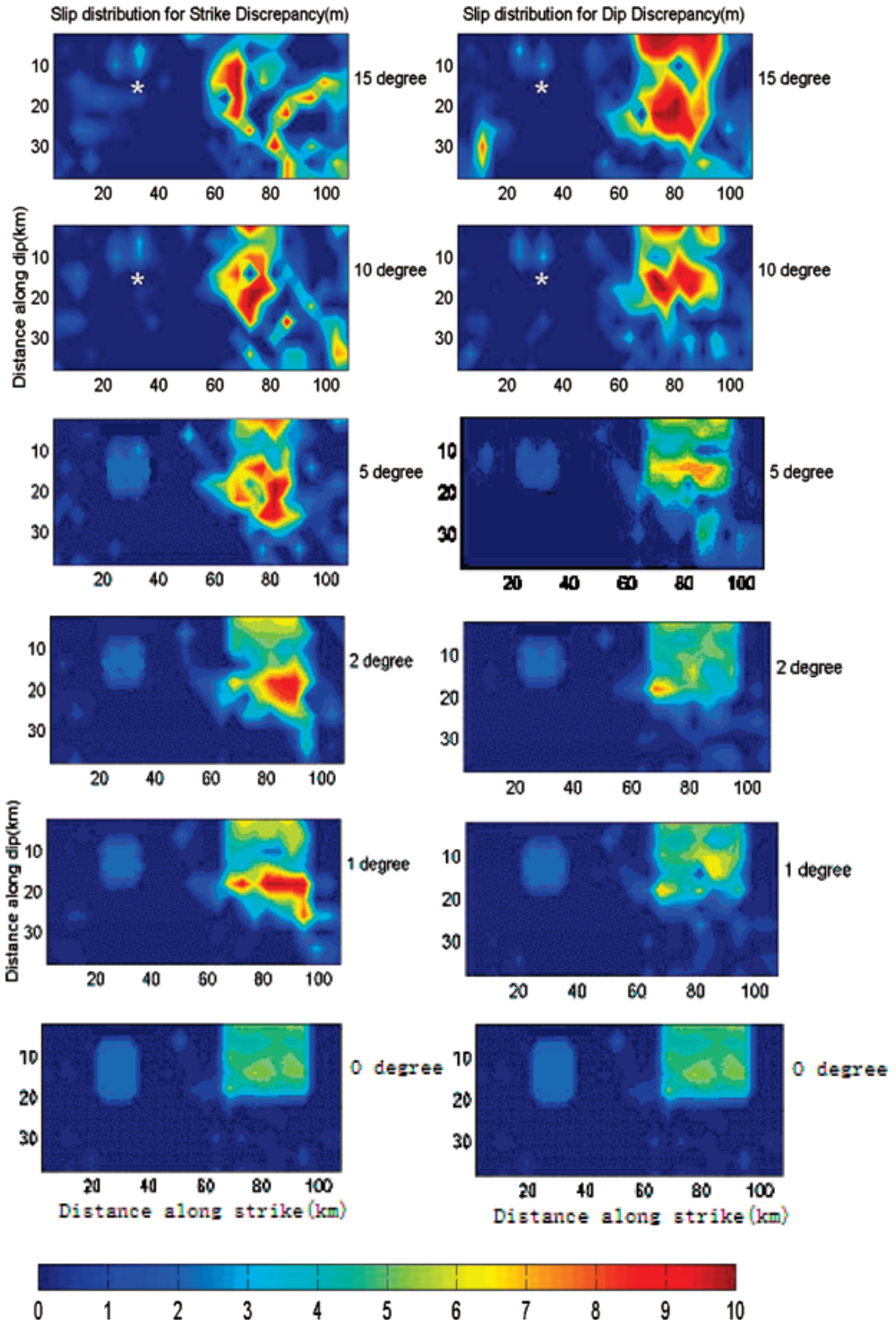


**Figure 10.** Inversion results when the strike or dip of the inversion rupture plane departs from that of the prescribed model by 15°, 10°, 5°, 2° and 1°.

the pre-set fault plane and the rupture timings of the points on the fault and source–time function the same as those of the original prescribed model in this analysis.

Ma *et al.* (2001) and Wu *et al.* (2001) respectively used two different media velocity structure models to calculate the Green's functions in their inversions for the Chi-Chi earthquake. The model of Ma *et al.* model was the average velocity structure of western Taiwan inferred from the works of Change *et al.* (2000) and Chen *et al.* (1998); this was used to calculate the 'data' in the numerous tests of this paper. Two different velocity structures for stations in the hanging wall or the footwall of the Chelupu fault were used in the model of Wu *et al.*. Fig. 12 shows all three velocity structures.

Fig. 12 indicates that these three velocity models (depth between 0 and 30 km) are similar in their gross features, but small differences exist. The difference between these velocity profiles provides a measure of the uncertainty that currently exists in our knowledge

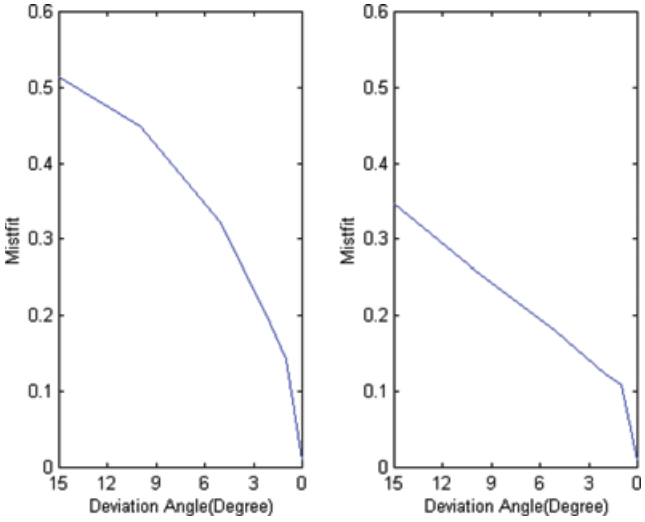


**Figure 11.** Waveform fitting error variation on the dip angle deviation and strike azimuth deviation.

of the actual velocity structure of Chi-Chi region. Differences in the velocity profiles lead directly to differences in wave propagation effects, which can ultimately result in some degree of influence on the inversion of the earthquake rupture process. To analyse the influence of the uncertain velocity models and white noise contamination, we use the hanging-wall model of Wu *et al.* to calculate the Green's function matrix for numerous test models whose 'data' was generated with the model of Ma *et al.* and with 5 per cent random noise.

The inversion results indicate that the noise, whether it originates from the uncertainty of the velocity structure or from data contamination, would certainly affect the results. However, in the following inversion for the Chi-Chi earthquake, the influence might not be very serious: the discrepancy between the velocity structure model used and the actual one is small if we can take the difference between Ma *et al.*'s model and Wu *et al.*'s model as the measure of the uncertainty. The inversion results (Fig. 13) have recovered the main features of the original test models despite there being some differences between the velocity structure used in calculation of he Green's function matrix and the velocity structure used in the calculation of the 'data', and 5 per cent disturbance was randomly added into 'data'. But the difference between the inversion result and the prescribed source is big and cannot be ignored.

## 4 DISCUSSION AND CONCLUSION

The inversion tests in this paper show that the multitime window method is an effective method for inverting for a complex earthquake faulting process without assuming the form of the source–time function. Using a time window of shorter width is helpful for inverting for finer details of the earthquake faulting process. However, the shorter-width time window may require using a larger number of time windows and a larger number of time windows requires more data to constrain the possible trade-off between the slip and rupture timing front distribution on the fault. Some studies have discussed the problem of choosing a suitable number of multitime windows and have pointed out that the increase in number of multitime windows might reduce the misfit between the synthetic and observed waveforms. However, such an improvement might not originate from the inversion result approaching the real one and might not be statistically significant. They suggested that the AIC measure should be used to select a suitable number of multitime windows. Because inversion methods that recover the slip and rupture time simultaneously presume the form of the source–time function, their basic inversion formula contains fewer unknown variables than the multitime window method. The number of data required may be less in the simultaneous slip and rupture time inversion methods. However, the earthquake faulting process recovered by such methods may be distorted if the presumed form of the source–time function departs from the true form too much; we generally do not know exactly the correct form of the source–time function.

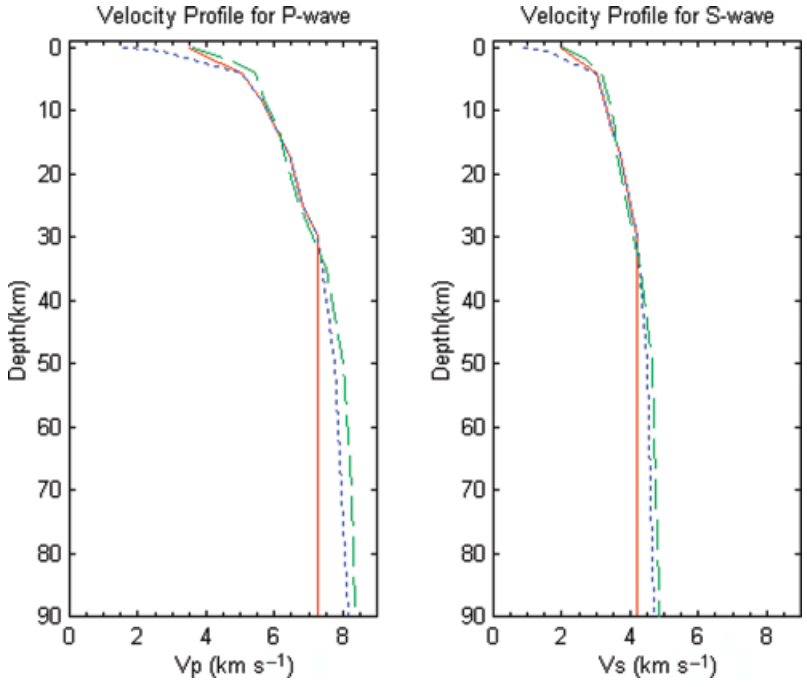


**Figure 12.** Velocity profiles for three regional media velocity model.

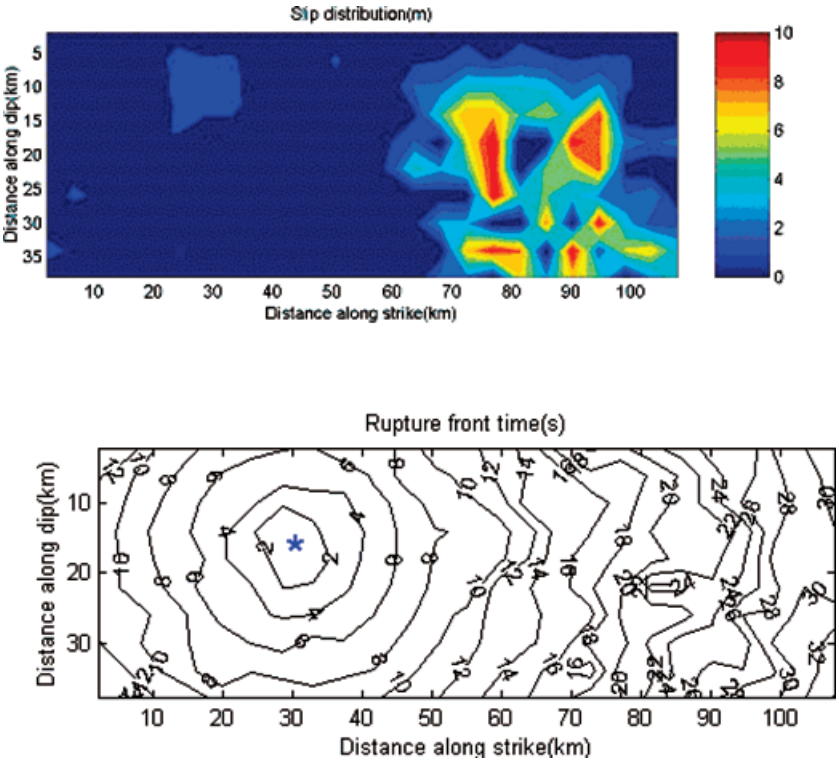


**Figure 13.** Inversion results when there are differences between the velocity structure used in calculation of Green's function matrix and the velocity structure used in calculation of 'data'.

Therefore, we suggest that the multitime window method is the better way to invert for the source history when the observation data are abundant. Otherwise, the simultaneous slip and rupture time inversion method may be considered if a reasonable source–time function form can be presumed

Teleseismic waves carry information about the source function only for that part of the space-time spectrum for which $|\omega/k| > c$, where $\omega$ is the angular frequency, $k$ is the wavenumber component in the fault plane, and $c$ is the wave-propagation velocity. So a complete determination of the source history requires observations near the seismic source (Aki & Richards 2002). As near-source data become more and more abundant, seismologists pay more and more attention to the use of near-source waveform data to invert for the source history. Our tests show that the near-source waveform data can recover the source history on the shallow part of the fault; however, they constrain the slip pattern poorly on the deep part of the fault. This is because the strength of the near-source ground motion strongly depends on the depth of the source. Information on the near-source ground motion from the deep part of the fault is too weak relative to that from the shallow part. There is not such an extreme difference between the shallow and deep parts in the teleseismic waveforms. In our test, jointly using one teleseismic station along with data in the near-source region can help to recover the correct faulting pattern on the whole fault. So, jointly using near-source and teleseismic waveform data may provide more complete information on the rupture process of the whole fault. In fact, the real improvement in the inversion resolution may come from directly combining all available data, particularly seismic with geodetic data since the combination can offer a more broadband frequency range of observations than the individual seismic data sets (Ji *et al.* 2001). Also, the static data (static component of the seismic data or GPS geodetic data) are particularly helpful for reducing the trade-off between timing and slip distribution. However, there are two main difficulties in such a combination:

(1) The static component of the seismic data is not easy to extract from the waveform data because of the baseline errors created by instrumental fatigue, instrumental tilting due to the strong ground distortion, waveform incompleteness, etc. It is known that the Chi-Chi earthquake was well recorded by an excellent local broadband (50 Hz dc) digital network with more than 600 stations. But the permanent dc component displacements can still hardly be recovered, and none of the papers about the source history inversions of the Chi-Chi earthquake (Ma *et al.* 2001; Wu *et al.* 2001; Zeng & Chen 2001) have used such data in their inversions.

(2) GPS data for most earthquakes are obtained after the earthquakes; GPS data are not a continuous recording and do not contain just the co-seismic static displacement. If the GPS were a continuous recording and its working time fortunately covered the earthquake source rupturing process, it would be very useful in source inversion research. Combined with the seismic data, the static displacement data from GPS are widely used in recent source history inversions, including those for the Chi-Chi earthquake (Ma *et al.* 2001; Wu *et al.* 2001; Zeng & Chen 2001). We suggest that at least one teleseismic waveform record should be added in order to constrain the faulting on the deep part of the fault when lots of near-source waveform data are used.

In the test on the influence of an uncertain strike or dip of the fault, we find that the near-source inversion result on the source is very sensitive to the strike and dip parameters of the presumed fault model. This is because so many stations in the test are very close to the up-dip projection of the fault radiation pattern node so that a slight error in the fault model plane can lead to erroneous inversion results. Our numerous tests also reaffirm that the

resolution of inversion results can be increased by improving the accuracy of the fault model by changing the strike and dip angles of the presumed fault model. But this will be very difficult for inversions for strong earthquakes like the Chi-Chi earthquake with a very large and complex seismogenic fault, and cannot be exactly represented with one, or a few, simple planar faults. So, in practical research on large earthquake source inversions we should not choose stations which are too near the surface breaking trace of the fault in case the inversion result is overly sensitive to the fault model.

In the tests on the influence of an uncertain velocity structure, we find that the uncertainty in structure for the Chi-Chi earthquake might not be big enough to affect the main features of the inversion results. This is so if we can take the difference between the models of Ma *et al.* and Wu *et al.* model as a measure of the uncertainty and other more detailed differences between the inversion patterns are ignored.

The Gauss iteration algorithm with non-negative constraint is used in the inversions for different tests. The results show that the inversion solutions are stable even though we have used different observation data (with different sampling intervals, different time lengths, different station combinations, with 5 per cent white noise, and so on). The Gauss algorithm needs much less memory and much less computation than the NNLS method. The Gauss algorithm will show a more obvious advantage relative to NNLS when the number of equations (eq. 2 in this paper) increases due to a larger number of multitime windows that need to be assumed.

## ACKNOWLEDGMENTS

This work has received constructive input from a number of people. In particular, we would like to thank Dr D. Wald, Dr R. Robinson and Dr K. Ma for their kind reviews and helpful suggestions.

The research was jointly supported by the National Natural Science Foundation of China (NSFC) under grants number 40174015 and 40134010. Part of this work was done in DPRI, Kyoto University, Japan.

## REFERENCES

Akaike, H., 1980. Likelihood and the Bayes procedure, in, *Bayesian Statistics*, pp. 143–166, eds Bernardo, J.M., Degroot, M.H., Lindley, D.V. & Smith, A.F.M., University Press, Valencia.

Aki, K. & Richards, P.G., 2002. *Quantitative Seismology*, 2nd edn, p. 516, University Science Books, Sausalito, CA.

Beroza, G.C. & Spudich, P., 1988. Linearized inversion for fault rupture behavior: application to the 1984 Morgan Hill, California, earthquake, *J. Geophys. Res.,* **93**, 6275–6296.

Bouchon, M., 1997. The state of stress on some faults of the San Andreas system as inferred from near-field strong motion data, *J. geophys. Res.,* **102**, 11 731–11 744.

Bouchon, M. & Ihmle, P., 1999. Stress drop and frictional heating during the 1994 deep Bolivia earthquake, *Geophys. Res. Lett.,* **26**, 3521–3524.

Change C.H., Wu, Y.M., Shin, T.C. & Wang, C.Y., 2000. Relation of the 1999 Chi-Chi earthquake in Taiwan, *Terr. Atmos. Ocean Sci.,* **11**, 581–590.

Chen C.-H., Teng, T.L. & Gung, Y.C., 1998. Ten-second Love wave propagation and strong ground motions in Taiwan, *J. geophys. Res.,* **103**, 21 253–21 273.

Chen, X., 1993. A systematic and efficient method of computing normal mode for multi-layered half-space, *Geophys, J. Int.,* **115**, 391–409.

Chen, X., 1999. Seismograms synthesis in multi-layered half-space (I). Theoretical formulation, *Earthquake Res. in China,* **13**, 1–11.

Chen, Y.G., Chen, W.S., Lee, J.C., Lee, Y.H., Lee, C.T., Chang, H.C. & Lo, C.H., 2001. Surface rupture of the 1999 Chi Chi earthquake yields insights on active tectonics of central Taiwan, *Bull. seism. Soc. Am.,* **91**, 977–985.

Dalguer, L.A., Irikura, K., Riera, J.D. & Chiu, H.C., 2001a. The importance of the dynamic source effects on strong ground motion during the 1999 Chi-Chi, Taiwan, earthquake: brief interpretation of the damage distribution on buildings, *Bull. seism. Soc. Am.,* **91**, 1112–1127.

Dalguer, L.A., Irikura, K. & Riera, J.D., 2001b. Fault dynamic rupture simulation of the hypocenter area of the thrust fault of the 1999 Chi-Chi (Taiwan) earthquake, *Geophys. Res. Lett.,* **28**, 1327–1330.

Day, S.M., 1982. Three-dimensional finite difference simulation of fault dynamics: rectangular faults with fixed rupture velocity, *Bull. seism. Soc. Am.,* **72**, 705–727.

Fukuyama, E. & Irikura, K., 1986. Rupture process of the 1983 Japan Sea (Akita-Oki) earthquake using a waveform inversion method, *Bull. seism. Soc. Am.,* **76**, 1623–1640.

Graves, R.W. & Wald, D.J., 2001. Resolution analysis of finite fault source inversion using one- and three-dimensional Green's functions 1. Strong motions, *J. geophys. Res.,* **106**, 8745–8766.

Hartzell, S., 1989. Comparison of seismic waveform inversion results for the rupture history of a fault—application to the 1986 North Palm Springs, California, earthquake, *J. geophys. Res.,* **94**, 7515–7534.

Hartzell, S.H. & Heaton, T.H., 1983. Inversion of strong ground motion and teleseismic waveform data for the fault rupture history of the 1979 Imperial Valley, California earthquake, *Bull. seism. Soc. Am.*.

Hartzell, S. & Liu, P., 1996. Calculation of earthquake rupture histories using a hybrid global search algorithm: application to the 1992 Landers, California, earthquake, *Phys. Earth planet. Int.,* **95**, 79–99. **73**, 1553–1583.

Ide, S., 2001. Complex source processes and the interaction of moderate earthquakes during the earthquake swarm in the Hida Mountains, Japan, 1998, *Tectonophysics,* **334**, 35–54.

Ji, C., Helmberger, D.V., Song A., Ma, K.F. & Wald, D.J., 2001. Slip distribution and tectonic implication of the 1999 Chi-Chi, Taiwan, earthquake, *Geophys. Res. Lett.,* **28**, 4379–4382.

Lee, C.T., Kang, K.H., Cheng, C.T. & Liao, C.W., 2000. Surface rupture and ground deformation associated with the Chi-Chi, Taiwan earthquake, *Sino-Geotechnics,* **81**, 5–18.

Lee, W.H.K., Shin, T.C., Kuo, K.W., Chen, K.C. & Wu, C.F., 2001. Data files from 'CWB free-field strong motion data from the 21 September Chi Chi, Taiwan, earthquake', *Bull. seism. Soc. Am.,* **91**, 1390.

Ma, K.F., Mori, Jim, Lee, S.L. & Yu, S.B., 2001. Spatial and temporal distribution of slip for the 1999 Chi Chi, Taiwan, earthquake, *Bull. seism. Soc. Am.,* **91**, 1069–1087.

Miyatake, T. & Yamashita, T., 1995. Theoretical seismic source studies, 1995, *J. Phys. Earth,* **43**, 171–182.

Nakayama, W. & Takeo, M., 1997. Slip history of the 1994 Sanriku-Haruka-Oki, Japan, earthquake deduced from strong motion data, *Bull. seism. Soc. Am.,* **87**, 918–931.

Nakumura, H. & Miyatake, T., 2000. An approximate expression of slip velocity time function for simulation of near-field strong ground motion, *Seismology,* **53**, 1–9(in Japanese).

Ohnaka, M. & Yamashita, T., 1989. A cohesive zone model for dynamic shear faulting based on experimentally inferred constitutive relation and strong motion source parameters, *J. geophys. Res.,* **94**, 4089–4104.

Okada, T., Umino, N., Ito, Y., Matsuzawa, T., Hasegawa, A. & Kamiyama, M., 2001. Source processes of 15 September 1998 *M* 5.0 Sendai, northeastern Japan, earthquake and its, M 3.8 foreshock by waveform inversion, *Bull. seism. Soc. Am.,* **91**, 1607–1618.

Olson, A.H. & Anderson, J., 1988. Implications of frequency-domain inversion of earthquake ground motions for resolving the space-time dependence of slip on an extended fault, *Geophys. J. R. astr. Soc.,* **94**, 443–455.

Olson, A.H. & Apsel, R.J., 1982. Finite faults and inverse theory with applications to the 1979 Imperial Valley earthquake, *Bull. seism. Soc. Am.,* **72**, 1969–2001.

Sekiguchi, H. & Iwata, T., 2002. Rupture process of the 1999 Kocaeli, Turkey, earthquake estimated from strong-motion waveforms, *Bull. seism. Soc. Am.,* **92**, 300–311.

Sekiguchi, H., Irikura, K. & Iwata, T., 2000. Fault geometry at the rupture termination of the 1995 Hyogo-ken Nanbu earthquake, *Bull. seism. Soc. Am.,* **90**, 117–133.

Shibazaki, B., Yoshida, Y. & Nakamura, M., 2001. Rupture nucleations in the 1995 Hyogo-ken Nanbu earthquake and its large aftershocks, *Geophys. J Int.,* **149**, 572–588.

Wald, D.J. & Heaton, T.H., 1994. Spatial and temporal distribution of slip for the 1992 Landers, California, earthquake, *Bull. seism. Soc. Am.,* **84**, 668–691.

Wu, C., Takeo, M. & Ide, S., 2001. Source process of the Chi Chi earthquake: a joint inversion of strong motion data and global positioning system data with a multifault model, *Bull. seism. Soc. Am.,* **91**, 1144–1157.

Xu, L.S., 1995. Study on the temporal and spatial process of the seismic source faulting, *PhD dissertation*, Institute of Geophysics, Chinese Seismological Bureau (in Chinese).

Yagi, Y. & Kikuchi, M., 2000. Source rupture process of the Chi-Chi, Taiwan, earthquake of 1999, obtained by seismic wave and GPS data, *2000 Western Pacific Geophysics Meeting,* WP104, Am. Geophys. Union, Tokyo.

Zeng, Y.H. & Anderson, J.G., 1996. A composite source modeling of the 1994 Northridge earthquake using genetic algorithm, *Bull. seism. Soc. Am.,* **86**, 871–883.

Zeng, Y.H. & Chen, C.H., 2001. Fault rupture process of the 20 September 1999 Chi-Chi, Taiwan, earthquake, *Bull. seism. Soc. Am.,* **91**, 1088–1098.

Zhou, S.Y. & Chen, X.F., 2003. Inversion of near-field waveform data for earthquake source rupture process(I): Method and numerical test, *Sci. China (D),* **46**, 1089–1102.